



HAL
open science

Bax is activated during rotavirus-induced apoptosis through the mitochondrial pathway.

Sandra Martin-Latil, Laurence Mousson, Arnaud Autret, Florence Colbère-Garapin, Bruno Blondel

► **To cite this version:**

Sandra Martin-Latil, Laurence Mousson, Arnaud Autret, Florence Colbère-Garapin, Bruno Blondel. Bax is activated during rotavirus-induced apoptosis through the mitochondrial pathway.. Journal of Virology, 2007, 81 (9), pp.4457-64. 10.1128/JVI.02344-06 . pasteur-00146502

HAL Id: pasteur-00146502

<https://pasteur.hal.science/pasteur-00146502>

Submitted on 16 Sep 2008

HAL is a multi-disciplinary open access archive for the deposit and dissemination of scientific research documents, whether they are published or not. The documents may come from teaching and research institutions in France or abroad, or from public or private research centers.

L'archive ouverte pluridisciplinaire **HAL**, est destinée au dépôt et à la diffusion de documents scientifiques de niveau recherche, publiés ou non, émanant des établissements d'enseignement et de recherche français ou étrangers, des laboratoires publics ou privés.

1 **Bax is activated during rotavirus-induced apoptosis through the**
2 **mitochondrial pathway**

3
4 Sandra Martin-Latil*, Laurence Mousson, Arnaud Autret, Florence Colbère-Garapin,
5 and Bruno Blondel

6
7 Unité de Biologie des Virus Entériques, Institut Pasteur, 25 rue du Docteur Roux, 75724 Paris
8 cedex 15, France

9
10 *Corresponding author :

11 Dr. Sandra Martin-Latil, Unité de Biologie des Virus Entériques, Institut Pasteur, 28 rue du
12 Docteur Roux, 75724 Paris cedex 15, France. Phone: (33) 1.40.61.35.90; Fax: (33)
13 1.40.61.34.21; E-mail: smartin@pasteur.fr

14
15 Running title: rotavirus induces Bax-dependent apoptosis

16
17 Word count abstract : 167

18 Word count manuscript without references, footnotes, figure legends : 4418

19 **ABSTRACT**

20

21 Rotaviruses are the leading cause of infantile viral gastroenteritis worldwide. Mature
22 enterocytes of the small intestine infected by rotavirus undergo apoptosis and their
23 replacement by less differentiated dividing cells probably leads to defective absorptive
24 function of the intestinal epithelium, and this contributes to osmotic diarrhea and rotavirus
25 pathogenesis.

26 Here, we show that the infection of MA104 cells by the simian rhesus rotavirus strain RRV
27 induced caspase-3 activation, DNA fragmentation and cleavage of poly(ADP-ribose)
28 polymerase (PARP); all three phenomena are features of apoptosis. RRV induced the release
29 of cytochrome c from mitochondria to the cytosol indicating that the mitochondrial apoptotic
30 pathway was activated. RRV infection of MA104 cells activated Bax, a proapoptotic member
31 of the Bcl-2 family, as revealed by its conformational change. Most importantly, Bax-specific
32 small interfering RNAs partially inhibited the cytochrome c release in RRV-infected cells.
33 Thus, mitochondrial dysfunction induced by rotavirus is Bax-dependent. Apoptosis
34 presumably leads to impaired intestinal functions, so our findings contribute to improve our
35 understanding of rotavirus pathogenesis at the cellular level.

36 INTRODUCTION

37

38 Rotavirus is a nonenveloped, double-stranded RNA virus belonging to the *Reoviridae*
39 family. It is the major etiologic agent of severe gastroenteritis in children under 5 years of age
40 and causes 600,000 deaths per year (40). Rotavirus infection is mainly restricted to the small
41 intestinal villus epithelium, resulting in villus atrophy. Diarrhea associated with rotavirus is a
42 multifactorial process: it involves dysfunctions of both nutrient digestion and enterocyte
43 absorption at the top of villi, and the secretion of water and electrolytes (29, 32, 43). The
44 defective absorptive function and the increased intestinal permeability may be a consequence
45 of the replacement of rotavirus-infected mature enterocytes by less differentiated cells and
46 this could contribute to rotavirus pathogenesis. In a murine model, rotavirus-infected
47 enterocytes undergo apoptosis and are therefore lost (4). It is therefore likely that apoptosis
48 makes a major contribution to diarrhea associated with rotavirus infection.

49 Cell death by apoptosis is part of the normal development and maintenance of homeostasis
50 (51) but is also involved in pathological situations associated with infections (16, 45) and
51 other (3) causes. Apoptosis is characterized by chromatin condensation, cell shrinkage,
52 membrane blebbing, and DNA fragmentation. It can be generally divided into two
53 nonexclusive pathways, the death receptor pathway (extrinsic) and the mitochondrial pathway
54 (intrinsic) (10, 13, 20). In the extrinsic pathway, stimulation of death receptors, such as Fas
55 and TNF receptor 1, leads to formation of the death-inducing signaling complex (DISC)
56 which allows the activation of caspase-8 and/or caspase-10, and then to that of downstream
57 effector caspases, particularly caspase-3 (2, 34). The intrinsic pathway is initiated in response
58 to diverse apoptotic stimuli and leads to the loss of mitochondrial transmembrane potential
59 and the release of several pro-apoptotic proteins, including cytochrome c and Smac/Diablo,
60 from the mitochondrial intermembrane space to the cytosol. Once released, cytochrome c

61 forms a complex with Apaf-1 and pro-caspase 9, resulting in activation of this initiator
62 caspase, and then of effector caspases (52). Smac/Diablo promotes caspase activation by
63 directly binding to and inhibiting the caspase inhibitors of the IAP family (50, 52). This
64 mitochondrial apoptotic pathway is tightly controlled by protein members of the Bcl-2 family.
65 Some, including Bcl-2 and Bcl-X_L, inhibit apoptosis, whereas others, including Bax and Bid,
66 induce apoptosis (9).

67 The extrinsic and intrinsic pathways may cross-talk through the pro-apoptotic protein Bid.
68 Indeed, caspase-8 can cleave Bid to generate a truncated form, tBid that targets mitochondria
69 and activates the pro-apoptotic protein Bax (26, 27, 30).

70 There have been very few studies of rotavirus-induced apoptosis in primate cells *in vitro*. An
71 early study in human carcinoma HT29 cells indicated that rotavirus induced peripheral
72 condensation of the chromatin and fragmentation of the nuclei, suggesting that apoptosis was
73 induced in infected cells (47). A more recent study in fully differentiated Caco-2 cells
74 indicated that rotavirus induced apoptosis in these cells, and did so through the mitochondrial
75 pathway (7). However, the precise signaling pathways leading to mitochondrial dysfunction
76 following rotavirus infection have not been investigated.

77 Here, we studied apoptosis induced by the Rhesus Rotavirus (RRV) strain in the monkey
78 kidney MA104 cells, the cellular model in which the rotavirus cycle has been best
79 characterized. We first confirmed that RRV-induced apoptosis in this model occurs through
80 the mitochondrial pathway as observed in Caco-2 cells. We then investigated the cascade of
81 events related to mitochondrial dysfunction. We report here that mitochondrial apoptotic
82 pathway in RRV-infected MA104 cells is Bax-dependent. It is, to our knowledge, the first
83 demonstration of Bax-dependent apoptosis in rotavirus-infected cells.

84 MATERIALS AND METHODS

85

86 Materials – Chemicals

87 Protein G (P3296), Staurosporine (S4400) and mouse anti-tubulin antibody (T5168) were
88 obtained from Sigma-Aldrich. Complete™ protease inhibitor mixture was obtained from
89 Roche Applied Science. z-VAD-fmk (627610), z-DEVD-fmk (264155) and z-LEHD-fmk
90 (218761) were purchased from Calbiochem. Mouse anti-CoxIV (A21347) antibody was
91 purchased from Molecular Probes. Mouse anti-Bcl-2 (sc-509) and anti-Bax (clone 6A7, sc-
92 23959) antibodies were purchased from Santa Cruz Biotechnology. Rabbit anti-Bax antibody
93 (NT 06-499) and mouse anti-cytochrome c antibody (556433) were obtained from Upstate
94 and BD Pharmingen, respectively. Rabbit anti-Smac/Diablo (2409) was purchased from
95 ProSci incorporated. Anti-mouse (NA9310V) and anti-rabbit (NA9340V) HRP-conjugated
96 secondary antibodies were obtained from Amersham Biosciences. Goat anti-Bid antibody
97 (AF860) and donkey anti-goat (HAF109) HRP-conjugated antibody were purchased from
98 Research & Diagnostic. Mouse anti-PARP antibody (clone C-2-10) was obtained from
99 Biomol. Mouse anti-Caspase-3 (9668) and anti-caspase-8 (9746) antibodies, and Bax (6321)
100 and non-targeted control (6201) siRNAs were purchased from Cell Signaling.

101

102 Cells and Virus

103 The monkey kidney MA104 cell line (MA104 cells) was cultured in minimum Eagle's
104 medium (MEM) supplemented with 10% fetal bovine serum (FBS), 2 mM glutamine and 0.1
105 mM non-essential amino acids, in a 5% CO₂ incubator. The rotavirus RRV strain was kindly
106 provided by Didier Poncet (Gif-sur-Yvette, France). Virus stocks were generated in MA104
107 cells in a serum-free culture medium supplemented with trypsin (0.5 μg/ml). Viruses were
108 activated by treatment with trypsin at 37°C for 30 min, and MA104 cell monolayers were

109 infected at a multiplicity of infection (m.o.i.) of 0.002 plaque-forming units/cell. After 1 h of
110 adsorption at 37°C, the inoculum was removed and the infected cells were incubated in
111 serum-free medium containing trypsin. When cytopathic effects were complete, the cultures
112 were frozen and then thawed, and the cell debris was removed by centrifugation.

113 To infect MA104 cells, RRV was activated in serum-free medium with 0.5 µg/ml trypsin.
114 Cells were washed twice in serum-free medium and then infected at an m.o.i of 10. The
115 inoculum was removed 1 h later and replaced with medium containing 10% FBS. This time
116 was defined as 0 h post-infection for all experiments.

117

118 **Assessment of apoptosis by flow cytometry**

119 The percentages of cells that were apoptotic was determined by flow cytofluorimetric analysis
120 of aliquots of 2×10^6 cells incubated with acridine orange (AO), a metachromatic nuclear dye
121 ($\lambda_{Ex_{max}}$: 500 nm, $\lambda_{Em_{max}}$: 526 nm), for 15 min at 37°C. AO fluorescence was measured with
122 a FACScan machine (Becton Dickinson). Two populations of cells were separated, one
123 consisting of the living cells characterized by a bright fluorescence labeling, and the second
124 being apoptotic cells with a characteristic distinct pattern of reduced fluorescence intensity
125 (12). We analyzed at least 10,000 cells for each sample. Data were analyzed with Cellquest
126 software (Becton Dickinson).

127

128 **Quantification of oligonucleosomal DNA fragmentation**

129 DNA fragmentation was assayed using a cell death detection ELISA kit (Roche Applied
130 Science) with RRV-infected MA104 cells plated in 6-well culture dishes according to the
131 manufacturer's instructions; the test measures the cytosolic histone-associated mono- and
132 oligonucleosome fragments. The concentration of nucleosomal fragments in cytosolic
133 fractions was determined by a sandwich enzyme-linked immunosorbent assay, using histone-

134 specific antibodies preadsorbed onto microtiter plates and peroxidase-conjugated antibodies
135 against DNA. Peroxidase activity was measured photometrically at 405 nm. The experiments
136 were run in triplicate.

137

138 **Detection of active caspase-8**

139 Caspase-8 activation was detected using a carboxyfluorescein FLICA apoptosis detection kit
140 (Immunochemistry Technologies, LLC) according to manufacturer's protocol. This assay is
141 based on a fluorescein-labeled inhibitor (FAM-LETD-fmk) that binds specifically to active
142 caspase-8. Apoptotic cells containing active caspase-8 were detected with a FACScan (Becton
143 Dickinson) machine. We analyzed at least 10,000 cells for each sample. Data were analyzed
144 with Cellquest software (Becton Dickinson).

145

146 **Transfection of small interfering RNA (siRNA)**

147 RNA interference was used to silence Bax gene expression in MA104 cells. Cells were plated
148 in 6-well culture dishes with complete medium and allowed to grow for 24 h, so as to reach
149 50–80% confluence. The cells were then transfected with siRNA (6321, Cell Signaling)
150 targeting Bax mRNA. An irrelevant siRNA (6201, Cell Signaling) that does not lead to the
151 specific degradation of any cellular mRNA was used as a negative control. A mixture of
152 OptiMEM medium and LipofectAMINE was incubated for 10 min at room temperature and
153 was then incubated with siRNA (25 nM) for 20 min at room temperature to allow complex
154 formation. This siRNA mixture was then added to each well following the manufacturer's
155 suggested protocol. Twenty-four hours after transfection, the medium was changed and cells
156 were infected with the virus 24 h later. Gene silencing was verified by testing for proteins by
157 immunoblot analysis after transient transfection of MA104 cells with siRNA.

158

159 **Whole cell extracts**

160 Approximately $5 \cdot 10^6$ cells were collected and washed with PBS, then resuspended in lysis
161 buffer (20 mM Tris pH 7.5, 135 mM NaCl, 2 mM EDTA, 1% Triton-X100, 10% glycerol)
162 supplemented with a protease inhibitor mixture (Roche). The cells were homogenized on ice
163 using dounce homogenizer and incubated for 10 min at 4°C in the lysis buffer. The lysates
164 were clarified by centrifugation for 10 min at 1200 g. The supernatant was collected as the
165 whole cell extract.

166

167 **Subcellular fractionation**

168 A subcellular proteome extraction kit (Calbiochem) was used to isolate cytosol and heavy
169 membrane fractions of MA104 cells according to the manufacturer's instructions. Cells
170 ($5 \cdot 10^6$) were harvested, pelleted, washed twice, resuspended in the ice-cold Extraction I buffer
171 containing a protease inhibitor mixture and incubated for 10 min at 4°C with gentle agitation.
172 The suspension was centrifuged at 1000 g at 4°C for 10 min. The supernatant was used as the
173 cytosol fraction. The pellet was resuspended in the ice-cold Extraction II buffer containing a
174 protease inhibitor mixture and incubated for 30 min at 4°C with gentle agitation. It was then
175 centrifuged at 6000 g for 10 min at 4°C, and the supernatant was used as the heavy membrane
176 fraction.

177

178 **Detection of Bax conformation change by immunoprecipitation**

179 Cells were harvested, washed in PBS and suspended in lysis buffer (10 mM hepes pH 7.4,
180 150 mM NaCl, 1% Chaps) containing a mixture of protease inhibitors. The zwitterionic
181 detergent Chaps was used because it does not affect Bax conformation (18). Cells were
182 homogenized on ice with dounce homogenizer, incubated for 2 h in the lysis buffer and
183 centrifuged for 30 min at 14000 g. The resulting supernatant was incubated overnight at 4°C

184 with 20 μ l of protein G and 2 μ g of the anti-Bax antibody (6A7). The immunoprecipitates
185 were collected by centrifugation at 14000 g (4°C, 5 min). The pellets were washed with
186 immunoprecipitation buffer and suspended in 50 μ l of Laemmli's buffer containing reducing
187 agent (Invitrogen).

188

189 **Western-blot analysis**

190 Protein concentrations were determined by using a Bio-Rad protein assay kit (Bio-Rad,
191 Richmond, CA). Samples of equal protein content were resuspended in Laemmli's
192 electrophoresis sample buffer containing reducing agent, denatured by boiling for 5 min,
193 subjected to SDS-PAGE (10-20% Tricine gels; Novex) and transferred to nitrocellulose
194 membranes (Amersham Biosciences). Nonspecific sites were blocked by incubating the
195 membranes for 1 h at room temperature with 5% nonfat milk and 0.1% Tween 20 in
196 Phosphate-Buffered Saline (PBST, pH 7.4), and the membranes were incubated overnight at
197 4°C or 2 h at room temperature with the primary antibody. Membranes were then washed in
198 PBST and treated with appropriate horse-radish peroxidase-conjugated secondary antibody
199 for 1 h at room temperature. The immunoblots were washed in PBST and developed using an
200 enhanced chemiluminescence detection kit (Amersham Biosciences). Anti-tubulin and Cox
201 IV antibodies were used to verify equal protein loading.

202

203 **Statistical Analysis**

204 Data are expressed as means \pm SEM of three independent experiments. Student's test was
205 used to compare experimental conditions and controls. A value of $P < 0.05$ was considered
206 significant.

207

208 **RESULTS**

209

210 **RRV infection induces apoptosis in MA104 cells through the mitochondrial pathway.**

211 Apoptosis induced by RRV in MA104 cells was investigated by following the kinetics of
212 DNA fragmentation with the Cell Death ELISA kit (Roche) (Fig. 1A). Early p.i. (until 8h
213 p.i.), DNA fragmentation was not significantly different in infected and uninfected cells.
214 Enrichment of nucleosomal DNA fragments started by 12 h p.i. and increased until 20 h p.i.
215 DNA fragmentation 20 h p.i. was 3-to 4-fold that of mock-infected cells and similar to that
216 observed after 14 h of treatment with staurosporine, used as positive control for DNA
217 fragmentation. These results confirm that rotavirus induced apoptosis in MA104 cells.

218 We then looked for activation of caspase-3, the central executioner in the apoptotic program,
219 in RRV-infected MA104 cells. Cleavage of 32 kDa procaspase-3 revealed by the detection, in
220 a whole cell lysate, of its 19 kDa cleavage product was substantial at about 14 h p.i. (Fig. 1B).
221 To confirm the activation of caspase-3 in RRV-infected MA104 cells, we investigated the
222 processing of one of its characteristic substrates, the poly(ADP-ribose) polymerase (PARP)
223 (Fig. 1B). The amount of full-length PARP in a whole lysate of RRV-infected MA104 cells
224 declined from 14 to 22 h p.i., thus paralleling the pattern of caspase-3 activation. These results
225 show that rotavirus induced caspase executioner activation in MA104 cells. Furthermore, the
226 peak of caspase-3 activation coincided with that of virus production during a single-cycle
227 infection in the same experimental conditions (data not shown).

228 To assess the role of caspases in cell death resulting from RRV infection, infected cells were
229 treated with a broad-spectrum caspase inhibitor, z-VAD-fmk (10 μ M, Calbiochem). The roles
230 of caspase-9 and caspase-3 were investigated with specific inhibitors, z-LEHD-fmk (10 μ M,
231 Calbiochem) and z-DEVD-fmk (10 μ M, Calbiochem), respectively. Apoptosis was analyzed
232 14 h p.i., by measuring chromatin condensation and fragmentation by flow cytometry after

233 Acridine Orange (AO) staining (Fig. 1C). The three caspase inhibitors significantly reduced
234 the percentage of apoptotic cells following RRV infection with respect to that in their
235 untreated counterparts. (The same level of apoptosis inhibition was observed with z-VAD-
236 fmk at a concentration of 100 μ M, data not shown). These results indicate that caspases are, at
237 least partly, involved in RRV-induced apoptosis. Furthermore, the decrease in apoptosis in
238 cells treated with the caspase 9 inhibitor seems to indicate that the mitochondrial pathway is
239 activated in RRV-infected cells.

240 To confirm that the mitochondrial pathway is activated during RRV infection in MA104 cells,
241 we investigated the kinetics of cytochrome c and Smac/Diablo efflux from mitochondria into
242 the cytosol. Infected cells were fractionated to separate the cytosolic fraction from the heavy
243 membrane fraction containing mitochondria, at various times after infection, and the fractions
244 were studied by western blotting (Fig. 2). Cytochrome c and Smac/Diablo were detected in
245 the cytoplasm of infected MA104 cells from 9 h p.i. and 12 h p.i., respectively: they increased
246 in amount in the the cytosol thereafter until the last time point investigated (18 h p.i.) whereas
247 they decreased in amount in the heavy membrane fraction. These findings indicate that
248 rotavirus causes the release of cytochrome c and Smac/Diablo into the cytosol in MA104
249 cells, consistent with apoptotic mitochondrial dysfunction.

250

251 **RRV-induced mitochondrial apoptotic pathway is caspases- and Bid-independent.**

252 We then looked for upstream signals that could trigger the activation of the mitochondrial
253 apoptotic pathway following RRV infection. This pathway can be activated by the BH3-only
254 protein Bid following its cleavage by caspase-8 (26, 30). First, the kinetics of the processing
255 of procaspase-8 was analyzed in RRV-infected MA104 cells, by immunoblotting (Fig. 3A).
256 The amounts of procaspase-8 decreased from 14 h p.i., relative to those in mock-infected
257 cells, suggesting caspase-8 activation. Caspase-8 activation was confirmed at 14 h p.i. by flow

258 cytometry with a FLICA apoptosis detection kit, based on the specific binding of a
259 fluorescein-labeled inhibitor (FAM-LETD-fmk, Immunochemistry Technologies, LLC) to
260 active caspase (Fig 3B). The kinetics of Bid processing was then analyzed in RRV-infected
261 MA104 cells, by immunoblotting (Fig. 3A). The amounts of Bid and procaspase-8, decreased
262 with respect to those in mock-infected cells, suggesting a cleavage of Bid mediated by
263 activated caspase-8.

264 To determine whether caspase-8 and Bid were required for engaging mitochondrial pathway
265 of apoptosis, we assessed cytochrome c release in the presence of the broad-spectrum caspase
266 inhibitor, z-VAD-fmk. The release of cytochrome c from the mitochondria into the cytosol in
267 RV-infected MA104 cells (14 h p.i.) was analyzed by western blotting following subcellular
268 fractionation (Fig. 4). As expected, cleavage of both Bid and PARP were inhibited in the
269 presence of the caspase inhibitor (Fig. 4A). In contrast, z-VAD-fmk was unable to prevent
270 cytochrome c release (Fig. 4B), suggesting that mitochondrial dysfunction in RRV-infected
271 MA104 cells is induced by a caspase- and Bid-independent mechanism. Thus, caspases seem
272 to be involved in RRV-induced apoptosis at a position in the pathway downstream from the
273 mitochondrial dysfunction.

274

275 **Bax is activated during RRV infection by a caspase independent pathway.**

276 The proapoptotic Bcl-2 family protein Bax is a pivotal regulator of cytochrome c release from
277 mitochondria to the cytosol (1, 38, 53). In healthy cells, most Bax is in the cytoplasm and in
278 an inactive form. Bax-mediated cell death occurs through a conformational change and its
279 translocation to the mitochondrial outer membrane, resulting in the loss of mitochondrial
280 membrane potential and the release of proapoptogenic factors including cytochrome c (18, 33,
281 54). We investigated kinetics of the conformational change of Bax in RRV-infected cells.
282 Total cell lysates were prepared at the indicated times post-infection (p.i) (Fig. 5A) in a lysis

283 buffer (containing Chaps) that did not affect Bax conformation. Bax was then
284 immunoprecipitated with an anti-Bax antibody (6A7) specific for the active conformation of
285 Bax (18, 19) and visualized by western blotting (Fig. 5A). In mock-infected cells, no activated
286 Bax was detected in the immunoprecipitates. From 12 h p.i, Bax was precipitated by antibody
287 6A7, indicating that RRV infection induced the conformational change of Bax as observed in
288 STS-treated cells used as positive control (data not shown). Thus, rotavirus infection triggers
289 a conformational change in Bax in MA104 cells. Furthermore, we showed that Bax activation
290 still occurred in the presence of the broad-spectrum caspase inhibitor, z-VAD-fmk (100 μ M,
291 Calbiochem) (Fig. 5B), indicating that Bax activation during RRV infection is caspase
292 independent.

293

294 **MA104 cell infection by RRV increases the Bax/Bcl-2 ratio.**

295 The Bcl-2-family, obviously, includes the antiapoptotic protein Bcl-2, which converges on
296 mitochondria and competes with proapoptotic Bax to regulate the release of cytochrome c in
297 response to apoptotic signal (1, 15, 44). As the ratio of pro- and anti-apoptotic proteins
298 determines, at least in part, the susceptibility of cells to the death signal (38), we studied the
299 time-dependent effects of RRV infection on Bax and Bcl-2 abundance in MA104 cells (Fig
300 5C). The amount of Bcl-2 decreased as the viral infection proceeded, whereas the total
301 amount of Bax was unaffected. Thus rotavirus infection increased the Bax/Bcl-2 ratio and this
302 could contribute to the mitochondrial apoptotic pathway by increasing the amount of free Bax
303 thereby allowing its activation.

304

305 **RRV-induced mitochondrial apoptotic pathway is Bax-dependent.**

306 These various findings seem to indicate that RRV induces Bax-mediated apoptosis in MA104
307 cells. To assess the requirement for Bax in RRV-induced mitochondrial dysfunction, MA104

308 cells were transiently transfected with specific small interfering RNA (siRNA) to knock down
309 Bax expression. Western blot analysis of MA104 cells transfected with the Bax siRNA (Cell
310 Signaling) and with the irrelevant control siRNA (Cell Signaling) confirmed that the specific
311 siRNA reduced significantly the abundance of Bax (50 %) (Fig 6A). We analyzed cytochrome
312 c release 14 h after infection of MA104 cells previously transfected with siRNA. Bax siRNA
313 partially inhibited cytochrome c release (52 %) in RRV-infected cells whereas the irrelevant
314 control siRNA had no effect. Furthermore, a much larger proportion of cytochrome c
315 remained in the membrane fraction containing mitochondria from RRV-infected cells treated
316 with Bax siRNA than from those treated with the irrelevant control (Fig 6B). We also
317 investigated RRV-induced apoptosis in MA104 cells, previously transfected with siRNA. The
318 fraction of apoptotic cells analyzed at 14 h p.i., by flow cytometry after Acridine Orange
319 (AO) staining, decreased in cells with reduced Bax expression (Fig. 6C). These results
320 demonstrate that Bax plays a key role in rotavirus-induced mitochondrial pathway of
321 apoptosis.

322

323 **DISCUSSION**

324

325 The pathophysiological mechanisms behind rotavirus-induced diarrhea have not been
326 completely described. In mice, apoptosis may be associated with functional changes during
327 rotavirus infection, particularly the modification of digestion and absorption functions.
328 Evidence for apoptosis has been reported in intestinal cell lines following rotavirus infection
329 *in vitro* (7, 47). However, the precise cellular and molecular mechanisms underlying
330 rotavirus-induced apoptosis have not been defined. Here, we investigated the apoptosis
331 induced by the RRV strain in MA104 cells, a monkey kidney epithelial cell line in which the
332 rotavirus cycle has been best characterized.

333 We showed that several hallmarks of apoptosis, notably DNA fragmentation, caspase-3
334 activation and PARP cleavage, were detected following RRV infection of MA104 cells. DNA
335 fragmentation was not observed in a previous study (6) in the same RRV-infected cells,
336 probably because of differences in the sensitivity of the tests used. Moreover, we report the
337 release of cytochrome c and Smac/DIABLO from mitochondria into the cytosol, implicating
338 mitochondrial dysfunction in the apoptotic pathway. Cytochrome c release is known to be the
339 pro-apoptotic signal causing the autocatalytic activation of procaspase-9 that triggers caspase-
340 3 cleavage. We showed that specific inhibition of either caspase-3 or caspase-9 reduced the
341 percentage of apoptotic cells following RRV infection. Thus, RRV-induced apoptosis is, at
342 least partly, dependent on caspase activation. It is also possible that Smac/Diablo is associated
343 with RRV-induced apoptosis through its action on cellular inhibitors of apoptosis proteins
344 (IAPs), as observed notably during reovirus-induced apoptosis (22).

345 We then investigated events upstream from RRV-induced mitochondrial dysfunction. We
346 focused on the Bcl-2 family proteins because they are central regulators of the mitochondrial
347 apoptotic pathway (1, 15, 35, 44) and have been implicated in various models of virus-
348 induced apoptosis (28, 36). Bax, one of the pro-apoptotic Bcl-2 family proteins, is the most
349 downstream activator molecule known of cytochrome c release machinery (42). We showed
350 that Bax is activated following RRV infection in MA104 cells: we detected its conformational
351 modification involving the exposure of its N-terminal extremity required for insertion into
352 mitochondrial membranes (18, 33). Once integrated into the outer mitochondrial membrane,
353 Bax can trigger cytochrome c release leading to the activation of the effector caspase-3 and
354 apoptotic cell death (11, 14, 23, 53). Our analysis of RRV-infected MA104 cells by using
355 siRNA-mediated gene silencing indicates, for the first time, that the apoptotic mitochondrial
356 pathway is activated through a Bax-dependent mechanism.

357 The inhibition of the prosurvival function of Bcl-2 is essential for the activation of Bax
358 because Bcl-2 can compete with Bax to regulate the release of cytochrome c (1, 15, 44). The
359 amount of antiapoptotic Bcl-2 protein decreased in RRV-infected cells without any change in
360 the amount of Bax. This results in an increase in the Bax/Bcl-2 ratio in RRV-infected cells
361 that could favor an increase in free Bax. Thus, one mechanism by which rotavirus may
362 contribute to Bax activation is by decreasing the number of Bax/Bcl-2 complexes at the
363 mitochondrial membrane.

364 Activated BH3-only proteins such as Bid can suppress the capacity of Bcl-2 to inhibit
365 apoptosis by interacting with it to displace and subsequently activate Bax (24, 25). Bid can be
366 activated by caspase-8, resulting in Bax activation and release of cytochrome c (23). We
367 showed that Bid processing was inhibited by the broad caspase inhibitor z-VAD-fmk in RRV-
368 infected cells; therefore rotavirus infection causes caspase-8 activation leading to Bid
369 activation. However, the inhibitor did not inhibit Bax activation and cytochrome c release,
370 suggesting that caspases and Bid do not play a crucial role in the Bax-dependent cytochrome
371 c release pathway during RRV infection. Thus, caspases seem to be involved in RRV-induced
372 apoptosis at a position in the pathway downstream from the mitochondrial dysfunction.

373 Several mechanisms for promoting Bax activation and mitochondrial dysfunction have been
374 described. These mechanisms include a signal transduction cascade involving mitogen-
375 activated protein kinases (MAPK) such as c-jun N-terminal protein kinase (JNK) and p38, as
376 described in other models (21, 49). The regulation of mitochondrial dysfunction by JNK
377 following virus infection was first demonstrated in reovirus-infected cells (8). Coulson *et al.*
378 (17) recently showed that JNK and p38, are activated by rotavirus infection in MA104 cells.
379 However the involvement of MAPK activation in Bax-dependent mitochondrial dysfunction
380 has not yet been demonstrated in rotavirus-infected cells.

381 Rotavirus infection of cultured cells induces a progressive rise in the cytosolic Ca^{2+}
382 concentration (5, 31, 46, 48). This increase may be involved in rotavirus-induced apoptosis,
383 and indeed, the intracellular calcium ion chelator BAPTA-AM partially inhibits apoptosis (7).
384 The rise in cytosolic Ca^{2+} concentration in rotavirus-infected cells results from a progressive
385 increase in plasma membrane permeability to Ca^{2+} and a depletion of endoplasmic reticulum
386 (ER) pools. Xu et al. showed that rotavirus infection leads to ER stress (55). This stress and
387 ER Ca^{2+} depletion may lead to Bax activation (39). It would be valuable to determine in
388 future studies whether rotavirus induces apoptosis by inducing both ER stress and ER Ca^{2+}
389 depletion leading to mitochondrial dysfunction. Several anti- and pro-apoptotic members of
390 the Bcl-2 family have been found, in addition to their mitochondrial localization, to be
391 associated to the ER and have been implicated in controlling apoptosis by affecting cellular
392 Ca^{2+} homeostasis (37, 39, 41). As demonstrated in this study, Bax is involved in
393 mitochondrial dysfunction in RRV infected-cells, but it could also be involved in ER Ca^{2+}
394 release and thus amplify the apoptotic signal in RRV-infected cells. It would therefore be
395 interesting to investigate whether Bax plays a role in ER Ca^{2+} release.

396 Apoptosis of mature rotavirus-infected enterocytes induces the replacement of these cells by
397 less differentiated dividing cells. This event may well be the cause of the defective absorptive
398 functions of the intestinal epithelial and consequently diarrhea associated with rotavirus
399 pathogenesis (4). Thus, the identification of the apoptotic signaling pathways in RRV-infected
400 cells would improve our understanding of the mechanisms by which rotavirus infection
401 causes functional alterations. Our demonstration of the activation of Bax during rotavirus
402 infection and its involvement in mitochondrial apoptotic pathway provide new insights
403 concerning rotavirus-induced pathogenesis.

404

405 **ACKNOWLEDGEMENTS**

406

407 We thank Didier Poncet (Gif-sur-Yvette, France) for the gift of MA104 cells and the rotavirus
408 RRV strain. We thank Isabelle Pelletier and Aure Saulnier for their help. This work was
409 supported by the Institut Pasteur, Danone Research Centre Daniel Carasso and the Ministère
410 de l'Education Nationale, de la Recherche et de la Technologie.

411

412 **REFERENCES**

413

- 414 1. **Adams, J. M., and S. Cory.** 2001. Life-or-death decisions by the Bcl-2 protein
415 family. *Trends Biochem Sci* **26**:61-6.
- 416 2. **Ashkenazi, A., and V. M. Dixit.** 1998. Death receptors: signaling and modulation.
417 *Science* **281**:1305-8.
- 418 3. **Blomgren, K., C. Zhu, X. Wang, J. O. Karlsson, A. L. Leverin, B. A. Bahr, C.**
419 **Mallard, and H. Hagberg.** 2001. Synergistic activation of caspase-3 by m-calpain
420 after neonatal hypoxia-ischemia: a mechanism of "pathological apoptosis"? *J Biol*
421 *Chem* **276**:10191-8.
- 422 4. **Boshuizen, J. A., J. H. Reimerink, A. M. Korteland-van Male, V. J. van Ham, M.**
423 **P. Koopmans, H. A. Buller, J. Dekker, and A. W. Einerhand.** 2003. Changes in
424 small intestinal homeostasis, morphology, and gene expression during rotavirus
425 infection of infant mice. *J Virol* **77**:13005-16.
- 426 5. **Brunet, J. P., J. Cotte-Laffitte, C. Linxe, A. M. Quero, M. Geniteau-Legendre,**
427 **and A. Servin.** 2000. Rotavirus infection induces an increase in intracellular calcium
428 concentration in human intestinal epithelial cells: role in microvillar actin alteration. *J*
429 *Virol* **74**:2323-32.

- 430 6. **Castilho, J. G., M. V. Botelho, F. Lauretti, N. Taniwaki, R. E. Linhares, and C.**
431 **Nozawa.** 2004. The in vitro cytopathology of a porcine and the simian (SA-11) strains
432 of rotavirus. *Mem Inst Oswaldo Cruz* **99**:313-7.
- 433 7. **Chaibi, C., J. Cotte-Laffitte, C. Sandre, A. Esclatine, A. L. Servin, A. M. Quero,**
434 **and M. Geniteau-Legendre.** 2005. Rotavirus induces apoptosis in fully differentiated
435 human intestinal Caco-2 cells. *Virology* **332**:480-90.
- 436 8. **Clarke, P., S. M. Meintzer, Y. Wang, L. A. Moffitt, S. M. Richardson-Burns, G.**
437 **L. Johnson, and K. L. Tyler.** 2004. JNK regulates the release of proapoptotic
438 mitochondrial factors in reovirus-infected cells. *J Virol* **78**:13132-8.
- 439 9. **Cory, S., and J. M. Adams.** 2002. The Bcl2 family: regulators of the cellular life-or-
440 death switch. *Nat Rev Cancer* **2**:647-56.
- 441 10. **Danial, N. N., and S. J. Korsmeyer.** 2004. Cell death: critical control points. *Cell*
442 **116**:205-19.
- 443 11. **Desagher, S., A. Osen-Sand, A. Nichols, R. Eskes, S. Montessuit, S. Lauper, K.**
444 **Maundrell, B. Antonsson, and J. C. Martinou.** 1999. Bid-induced conformational
445 change of Bax is responsible for mitochondrial cytochrome c release during apoptosis.
446 *J Cell Biol* **144**:891-901.
- 447 12. **Estaquier, J., T. Idziorek, F. de Bels, F. Barre-Sinoussi, B. Hurtrel, A. M.**
448 **Aubertin, A. Venet, M. Mehtali, E. Muchmore, P. Michel, and et al.** 1994.
449 Programmed cell death and AIDS: significance of T-cell apoptosis in pathogenic and
450 nonpathogenic primate lentiviral infections. *Proc Natl Acad Sci U S A* **91**:9431-5.
- 451 13. **Green, D. R., and G. Kroemer.** 2004. The pathophysiology of mitochondrial cell
452 death. *Science* **305**:626-9.

- 453 14. **Gross, A., J. Jockel, M. C. Wei, and S. J. Korsmeyer.** 1998. Enforced dimerization
454 of BAX results in its translocation, mitochondrial dysfunction and apoptosis. *Embo J*
455 **17:3878-85.**
- 456 15. **Gross, A., J. M. McDonnell, and S. J. Korsmeyer.** 1999. BCL-2 family members
457 and the mitochondria in apoptosis. *Genes Dev* **13:1899-911.**
- 458 16. **Hofman, P., and P. Auberger.** 2000. [Roles and mechanisms of apoptosis in
459 infectious diseases]. *Ann Pathol* **20:313-22.**
- 460 17. **Holloway, G., and B. S. Coulson.** 2006. Rotavirus Activates JNK and p38 Signaling
461 Pathways in Intestinal Cells, Leading to AP-1-Driven Transcriptional Responses and
462 Enhanced Virus Replication. *J Virol* **80:10624-33.**
- 463 18. **Hsu, Y. T., and R. J. Youle.** 1998. Bax in murine thymus is a soluble monomeric
464 protein that displays differential detergent-induced conformations. *J Biol Chem*
465 **273:10777-83.**
- 466 19. **Hsu, Y. T., and R. J. Youle.** 1997. Nonionic detergents induce dimerization among
467 members of the Bcl-2 family. *J Biol Chem* **272:13829-34.**
- 468 20. **Jin, Z., and W. S. El-Deiry.** 2005. Overview of cell death signaling pathways. *Cancer*
469 *Biol Ther* **4:139-63.**
- 470 21. **Kim, B. J., S. W. Ryu, and B. J. Song.** 2006. JNK- and p38 kinase-mediated
471 phosphorylation of Bax leads to its activation and mitochondrial translocation and to
472 apoptosis of human hepatoma HepG2 cells. *J Biol Chem* **281:21256-65.**
- 473 22. **Kominsky, D. J., R. J. Bickel, and K. L. Tyler.** 2002. Reovirus-induced apoptosis
474 requires mitochondrial release of Smac/DIABLO and involves reduction of cellular
475 inhibitor of apoptosis protein levels. *J Virol* **76:11414-24.**

- 476 23. **Korsmeyer, S. J., M. C. Wei, M. Saito, S. Weiler, K. J. Oh, and P. H. Schlesinger.**
477 2000. Pro-apoptotic cascade activates BID, which oligomerizes BAK or BAX into
478 pores that result in the release of cytochrome c. *Cell Death Differ* **7**:1166-73.
- 479 24. **Kuwana, T., L. Bouchier-Hayes, J. E. Chipuk, C. Bonzon, B. A. Sullivan, D. R.**
480 **Green, and D. D. Newmeyer.** 2005. BH3 domains of BH3-only proteins
481 differentially regulate Bax-mediated mitochondrial membrane permeabilization both
482 directly and indirectly. *Mol Cell* **17**:525-35.
- 483 25. **Letai, A., M. C. Bassik, L. D. Walensky, M. D. Sorcinelli, S. Weiler, and S. J.**
484 **Korsmeyer.** 2002. Distinct BH3 domains either sensitize or activate mitochondrial
485 apoptosis, serving as prototype cancer therapeutics. *Cancer Cell* **2**:183-92.
- 486 26. **Li, H., H. Zhu, C. J. Xu, and J. Yuan.** 1998. Cleavage of BID by caspase 8 mediates
487 the mitochondrial damage in the Fas pathway of apoptosis. *Cell* **94**:491-501.
- 488 27. **Li, S., Y. Zhao, X. He, T. H. Kim, D. K. Kuharsky, H. Rabinowich, J. Chen, C.**
489 **Du, and X. M. Yin.** 2002. Relief of extrinsic pathway inhibition by the Bid-dependent
490 mitochondrial release of Smac in Fas-mediated hepatocyte apoptosis. *J Biol Chem*
491 **277**:26912-20.
- 492 28. **Liu, Y., Y. Pu, and X. Zhang.** 2006. Role of the mitochondrial signaling pathway in
493 murine coronavirus-induced oligodendrocyte apoptosis. *J Virol* **80**:395-403.
- 494 29. **Lundgren, O., and L. Svensson.** 2001. Pathogenesis of rotavirus diarrhea. *Microbes*
495 *Infect* **3**:1145-56.
- 496 30. **Luo, X., I. Budihardjo, H. Zou, C. Slaughter, and X. Wang.** 1998. Bid, a Bcl2
497 interacting protein, mediates cytochrome c release from mitochondria in response to
498 activation of cell surface death receptors. *Cell* **94**:481-90.

- 499 31. **Michelangeli, F., M. C. Ruiz, J. R. del Castillo, J. E. Ludert, and F. Liprandi.**
500 1991. Effect of rotavirus infection on intracellular calcium homeostasis in cultured
501 cells. *Virology* **181**:520-7.
- 502 32. **Morris, A. P., and M. K. Estes.** 2001. Microbes and microbial toxins: paradigms for
503 microbial-mucosal interactions. VIII. Pathological consequences of rotavirus infection
504 and its enterotoxin. *Am J Physiol Gastrointest Liver Physiol* **281**:G303-10.
- 505 33. **Murphy, K. M., U. N. Streips, and R. B. Lock.** 2000. Bcl-2 inhibits a Fas-induced
506 conformational change in the Bax N terminus and Bax mitochondrial translocation. *J*
507 *Biol Chem* **275**:17225-8.
- 508 34. **Muzio, M., A. M. Chinnaiyan, F. C. Kischkel, K. O'Rourke, A. Shevchenko, J. Ni,**
509 **C. Scaffidi, J. D. Bretz, M. Zhang, R. Gentz, M. Mann, P. H. Krammer, M. E.**
510 **Peter, and V. M. Dixit.** 1996. FLICE, a novel FADD-homologous ICE/CED-3-like
511 protease, is recruited to the CD95 (Fas/APO-1) death--inducing signaling complex.
512 *Cell* **85**:817-27.
- 513 35. **Narita, M., S. Shimizu, T. Ito, T. Chittenden, R. J. Lutz, H. Matsuda, and Y.**
514 **Tsujimoto.** 1998. Bax interacts with the permeability transition pore to induce
515 permeability transition and cytochrome c release in isolated mitochondria. *Proc Natl*
516 *Acad Sci U S A* **95**:14681-6.
- 517 36. **Natoni, A., G. E. Kass, M. J. Carter, and L. O. Roberts.** 2006. The mitochondrial
518 pathway of apoptosis is triggered during feline calicivirus infection. *J Gen Virol*
519 **87**:357-61.
- 520 37. **Nutt, L. K., A. Pataer, J. Pahler, B. Fang, J. Roth, D. J. McConkey, and S. G.**
521 **Swisher.** 2002. Bax and Bak promote apoptosis by modulating endoplasmic reticular
522 and mitochondrial Ca²⁺ stores. *J Biol Chem* **277**:9219-25.

- 523 38. **Oltvai, Z. N., C. L. Milliman, and S. J. Korsmeyer.** 1993. Bcl-2 heterodimerizes in
524 vivo with a conserved homolog, Bax, that accelerates programmed cell death. *Cell*
525 **74:609-19.**
- 526 39. **Pan, Z., M. B. Bhat, A. L. Nieminen, and J. Ma.** 2001. Synergistic movements of
527 Ca(2+) and Bax in cells undergoing apoptosis. *J Biol Chem* **276:32257-63.**
- 528 40. **Parashar, U. D., C. J. Gibson, J. S. Bresse, and R. I. Glass.** 2006. Rotavirus and
529 severe childhood diarrhea. *Emerg Infect Dis* **12:304-6.**
- 530 41. **Pinton, P., and R. Rizzuto.** 2006. Bcl-2 and Ca²⁺ homeostasis in the endoplasmic
531 reticulum. *Cell Death Differ* **13:1409-18.**
- 532 42. **Puthalakath, H., and A. Strasser.** 2002. Keeping killers on a tight leash:
533 transcriptional and post-translational control of the pro-apoptotic activity of BH3-only
534 proteins. *Cell Death Differ* **9:505-12.**
- 535 43. **Ramig, R. F.** 2004. Pathogenesis of intestinal and systemic rotavirus infection. *J Virol*
536 **78:10213-20.**
- 537 44. **Reed, J. C.** 1998. Bcl-2 family proteins. *Oncogene* **17:3225-36.**
- 538 45. **Roulston, A., R. C. Marcellus, and P. E. Branton.** 1999. Viruses and apoptosis.
539 *Annu Rev Microbiol* **53:577-628.**
- 540 46. **Ruiz, M. C., J. Cohen, and F. Michelangeli.** 2000. Role of Ca²⁺ in the replication
541 and pathogenesis of rotavirus and other viral infections. *Cell Calcium* **28:137-49.**
- 542 47. **Superti, F., M. G. Ammendolia, A. Tinari, B. Bucci, A. M. Giammarioli, G.**
543 **Rainaldi, R. Rivabene, and G. Donelli.** 1996. Induction of apoptosis in HT-29 cells
544 infected with SA-11 rotavirus. *J Med Virol* **50:325-34.**
- 545 48. **Tian, P., M. K. Estes, Y. Hu, J. M. Ball, C. Q. Zeng, and W. P. Schilling.** 1995.
546 The rotavirus nonstructural glycoprotein NSP4 mobilizes Ca²⁺ from the endoplasmic
547 reticulum. *J Virol* **69:5763-72.**

- 548 49. **Tsuruta, F., J. Sunayama, Y. Mori, S. Hattori, S. Shimizu, Y. Tsujimoto, K.**
549 **Yoshioka, N. Masuyama, and Y. Gotoh.** 2004. JNK promotes Bax translocation to
550 mitochondria through phosphorylation of 14-3-3 proteins. *Embo J* **23**:1889-99.
- 551 50. **van Loo, G., X. Saelens, M. van Gurp, M. MacFarlane, S. J. Martin, and P.**
552 **Vandenabeele.** 2002. The role of mitochondrial factors in apoptosis: a Russian
553 roulette with more than one bullet. *Cell Death Differ* **9**:1031-42.
- 554 51. **Vaux, D. L., and S. J. Korsmeyer.** 1999. Cell death in development. *Cell* **96**:245-54.
- 555 52. **Wang, X.** 2001. The expanding role of mitochondria in apoptosis. *Genes Dev*
556 **15**:2922-33.
- 557 53. **Wei, M. C., W. X. Zong, E. H. Cheng, T. Lindsten, V. Panoutsakopoulou, A. J.**
558 **Ross, K. A. Roth, G. R. MacGregor, C. B. Thompson, and S. J. Korsmeyer.** 2001.
559 Proapoptotic BAX and BAK: a requisite gateway to mitochondrial dysfunction and
560 death. *Science* **292**:727-30.
- 561 54. **Wolter, K. G., Y. T. Hsu, C. L. Smith, A. Nechushtan, X. G. Xi, and R. J. Youle.**
562 1997. Movement of Bax from the cytosol to mitochondria during apoptosis. *J Cell*
563 *Biol* **139**:1281-92.
- 564 55. **Xu, A., A. R. Bellamy, and J. A. Taylor.** 1998. BiP (GRP78) and endoplasmic
565 (GRP94) are induced following rotavirus infection and bind transiently to an
566 endoplasmic reticulum-localized virion component. *J Virol* **72**:9865-72.

567

FIGURE LEGENDS

568

569 **Fig. 1. RRV induces apoptosis in MA104 cells.**

570 **A.** DNA-fragmentation in RRV-infected MA104 cells. At the indicated times post-infection,
571 DNA fragmentation was analyzed using the Cell Death Detection ELISA^{PLUS} assay which
572 detects the appearance of histone-associated low molecular weight DNA in the cytoplasm of
573 cells. Mock-infected and staurosporine (STS)-treated MA104 cells were used as negative and
574 positive controls, respectively. Enrichment Factor was calculated as the absorbance at
575 405/492 nm for treated cells divided by that of the corresponding untreated cells. Data are
576 means \pm S.D. of three experiments. *P<0.05 by Student t-test comparing RRV-infected
577 MA104 cells to mock-infected MA104 cells.

578 **B.** RRV infection triggered caspase-3 activation and PARP processing in MA104 cells. At the
579 indicated times post-infection, whole cell extracts were subjected to western blot analysis
580 with anti-caspase-3 and anti-PARP antibodies. Mock-infected MA104 cells were used as
581 negative controls. An asterisk (*) indicates a nonspecific protein band which was used as a
582 protein loading control. Positions of markers of molecular weight are indicated at the left of
583 panel.

584 **C.** RRV-induced apoptosis is dependent on caspases activation in MA104 cells. MA104 cells
585 were treated or non-treated with the broad caspase inhibitor z-VAD-fmk (10 μ M), the specific
586 caspase-9 inhibitor z-LEHD-fmk (10 μ M) or the specific caspase-3 inhibitor z-DEVD-fmk
587 (10 μ M) 2 h before RRV infection and maintained throughout the infection. Mock- and RRV-
588 infected MA104 cells were analyzed 14 h post-infection (p.i) by flow cytometry after acridine
589 orange nuclear dye staining and the fold increase of apoptosis was calculated as the ratio of
590 the apoptotic cell percentages for RRV-infected MA104 cells to that for mock-infected
591 MA104 cells. Data are expressed as means of three independent experiments. Error bars

592 represent the standard errors of the mean, *P<0.05 by Student t-test comparing non-treated
593 MA104 cells to treated MA104 cells.

594

595 **Fig. 2. Mitochondrial apoptotic pathway is activated in RRV-infected MA104 cells.**

596 Time course of cytochrome c and Smac/Diablo release in RRV-infected MA104 cells. At the
597 indicated times post-infection, cells were collected and subjected to subcellular fractionation
598 as described in Material and Methods. The cytosolic (C) and heavy membrane (HM) fraction
599 proteins were assayed by western blot analysis for cytochrome c and Smac/Diablo. Mock-
600 infected MA104 cells were used as negative controls. Cox IV and tubulin were used as
601 protein loading controls for heavy membrane and cytosolic fractions, respectively. Positions
602 of markers of molecular weight are indicated at the left of panel. Cytochrome c and
603 Smac/Diablo protein levels of heavy membrane and cytosolic fractions were determined by
604 densitometry and plotted as ratios relative to the levels of Cox IV and tubulin, respectively
605 (*lower panel*).

606

607 **Fig. 3. RRV induces caspase-8 activation and Bid processing in MA104 cells.**

608 **A.** Time course of caspase-8 activation and Bid processing in RRV-infected MA104 cells. At
609 the indicated times post-infection, whole cell extracts were subjected to immunoblot analysis
610 with anti-caspase-8 and anti-Bid antibodies. Mock-infected MA104 cells were used as
611 negative controls. Tubulin was used as a control for protein loading. Positions of markers of
612 molecular weight are indicated at the left of panel. Bid protein levels were determined by
613 densitometry and plotted as ratios relative to the levels of tubulin (*lower panel*).

614 **B.** Caspase-8 activation was determined in mock- and RRV-infected MA104 cells (14 h p.i.)
615 by flow cytometry using cell-permeable, fluorescein-labeled inhibitor (FAM-LETD-fmk), that
616 binds specifically on active caspase-8, as described in Material and Methods. Histogram

617 representative of two independent experiments is shown. The percentage of cells positive for
618 activated caspase-8 following RRV infection is indicated.

619

620 **Fig. 4. Cytochrome c release in RRV-infected MA104 cells is caspase-independent.**

621 **A.** The broad-spectrum caspase inhibitor z-VAD-fmk inhibits Bid and PARP processing in
622 RRV-infected MA104 cells. Mock- and RRV-infected MA104 cells were pretreated or not
623 pretreated with 100 μ M z-VAD-fmk for 2 h before and during RRV infection. Whole cell
624 extracts were prepared 14 h post-infection and Bid and PARP were assayed by western blot
625 analysis. Mock-infected MA104 cells were used as negative controls. Tubulin was used as a
626 control for protein loading. Positions of markers of molecular weight are indicated at the left
627 of panel.

628 **B.** z-VAD-fmk did not inhibit cytochrome c release in RRV-infected MA104 cells. Mock-
629 and RRV-infected MA104 cells were pretreated or not pretreated with 100 μ M z-VAD-fmk
630 for 2 h before and during infection. Fourteen hours after RRV infection, the cytosolic and
631 heavy membrane fractions were assayed for cytochrome c by western blotting. Mock-infected
632 MA104 cells were used as negative controls, Cox IV and tubulin were used as protein loading
633 controls for heavy membrane and cytosolic fractions, respectively. Positions of markers of
634 molecular weight are indicated at the left of panel.

635

636 **Fig. 5. RRV induces Bax protein activation in MA104 cells.**

637 **A.** RRV induced Bax conformational change in MA104 cells. At the indicated time post-
638 infection (p.i), MA104 cells were lysed in immunoprecipitation buffer containing the
639 zwitterionic detergent Chaps (which maintains Bax in its activated conformation). Anti-Bax
640 6A7 antibody was used to immunoprecipitate conformationally active Bax protein. The
641 immunoprecipitates were analyzed by immunoblotting with anti-Bax antibody.

642 Immunoglobulin light chains are indicated with an asterisk (*). Mock-infected MA104 cells
643 were used as negative control. Positions of markers of molecular weight are indicated at the
644 left of panel.

645 **B.** z-VAD-fmk did not inhibit Bax conformational change in RRV-infected MA104 cells.
646 RRV-infected MA104 cells were pretreated or not pretreated with 100 μ M z-VAD-fmk for 2
647 h before and during infection. Whole cell lysates were immunoprecipitated with activated Bax
648 antibody (clone 6A7) and then analyzed by immunoblotting with anti-Bax antibody. Mock-
649 infected MA104 cells were used as negative control. Immunoglobulin light chains are
650 indicated with an asterisk (*). Positions of markers of molecular weight are indicated at the
651 left of panel.

652 **C.** RRV infection promoted Bcl-2 degradation in MA104 cells. At the indicated times post-
653 infection, whole cell lysates were prepared. Bax and Bcl-2 proteins were detected by western
654 blotting with anti-Bax and anti-Bcl-2 specific antibodies. Mock-infected MA104 cells were
655 used as negative controls. Tubulin was used as a control for protein loading. Positions of
656 markers of molecular weight are indicated at the left of panel.

657

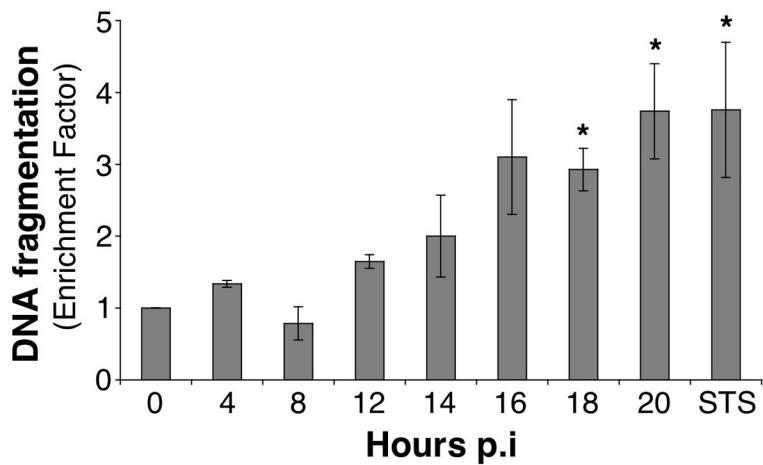
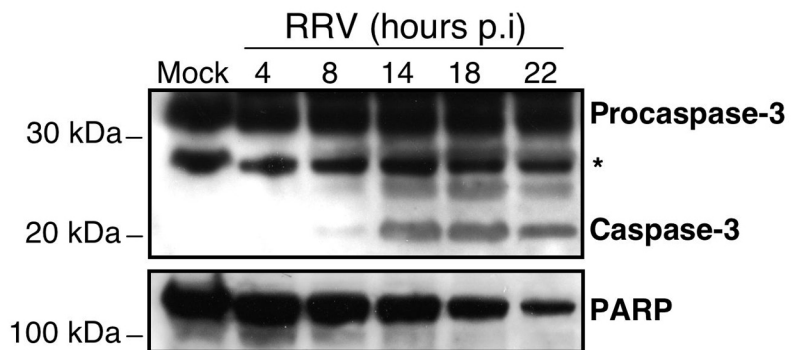
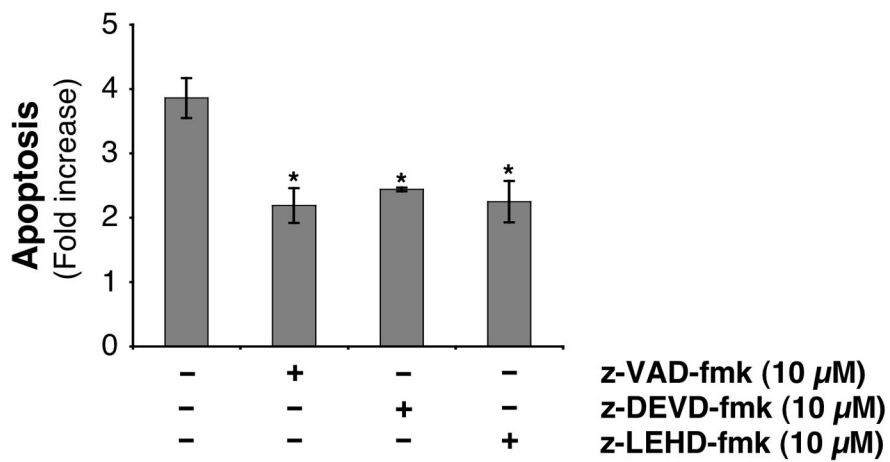
658 **Fig. 6. Cytochrome c release induced by RRV infection of MA104 cells is Bax-**
659 **dependent.**

660 **A.** Knock down of Bax expression in MA104 cells. Cells were transfected with specific Bax
661 siRNA or irrelevant siRNA. Bax protein was then assayed in whole cell lysates from by
662 immunoblotting. Levels of tubulin were used as protein loading controls (*upper panel*). Bax
663 protein levels were determined by densitometry and plotted as ratios relative to the levels of
664 tubulin. Positions of markers of molecular weight are indicated at the left of panel. The graph
665 shows the mean percentage of Bax expression inhibition in three independent experiments.
666 Error bars represent the standard errors of the mean, *P<0.05 by Student t-test comparing

667 irrelevant siRNA-transfected to Bax siRNA-transfected MA104 cells (*lower panel*).

668 **B.** siRNA-induced silencing of the Bax gene results in reduction of RRV-induced cytochrome
669 c release in MA104 cells. Cells were infected with RRV 48 h post-transfection and
670 cytochrome c was analyzed in cytosolic (C) and heavy membrane fractions (M) by western
671 blotting 14h post-infection. Mock-infected MA104 cells were used as negative controls.
672 Tubulin and Cox IV were used as controls for protein loading of cytosolic (C) and heavy
673 membrane (M) fractions, respectively. Positions of markers of molecular weight are indicated
674 at the left of panel. Cytochrome c protein levels of heavy membrane and cytosolic fractions
675 were determined by densitometry and plotted as ratios relative to the levels of Cox IV and
676 tubulin, respectively (*lower panel*).

677 **C.** siRNA-induced silencing of the Bax gene results in reduction of RRV-induced apoptosis in
678 MA104 cells. Cells were infected with RRV 48 h post-transfection and the percentage of
679 apoptosis was determined by flow cytometry after Acridine Orange (AO) staining. MA104
680 cells transfected with irrelevant siRNA was used as negative control.

A**B****C****Figure 1**

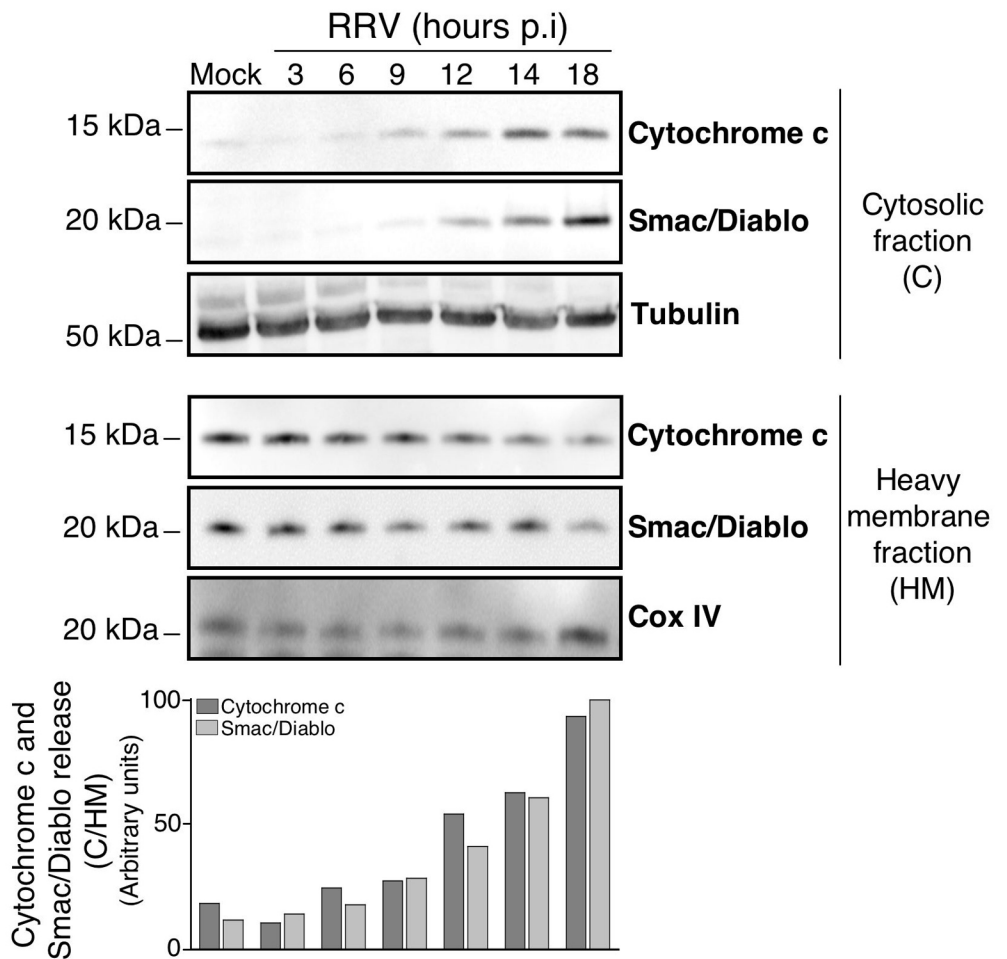
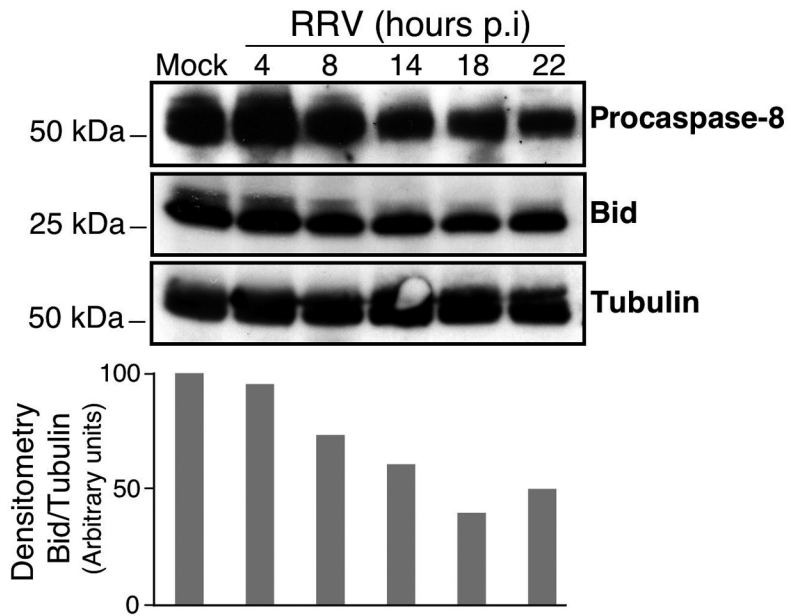
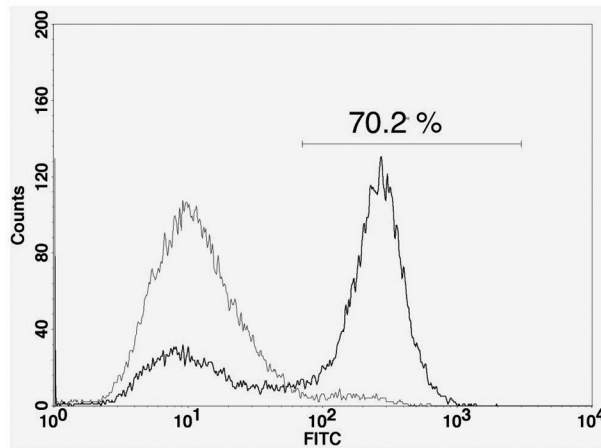
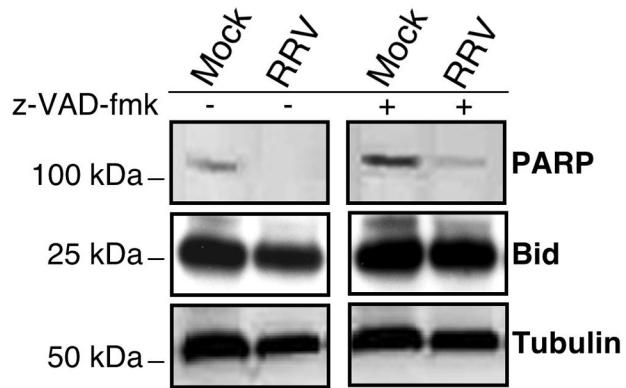
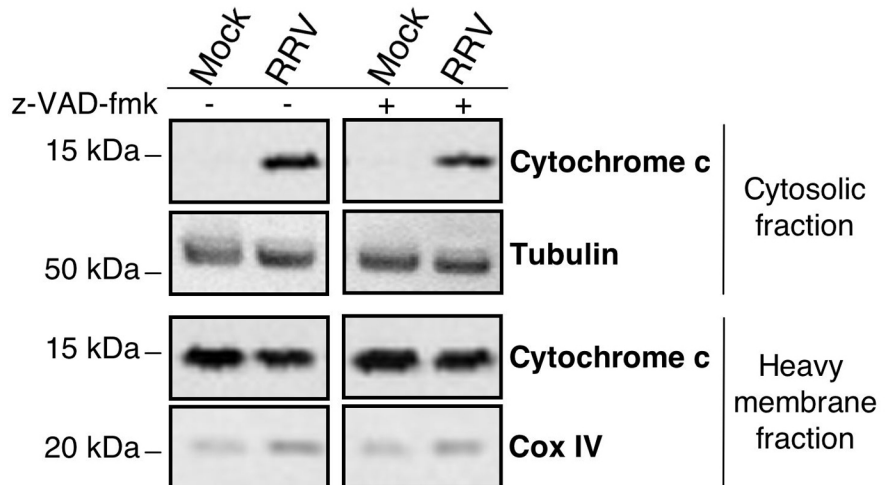
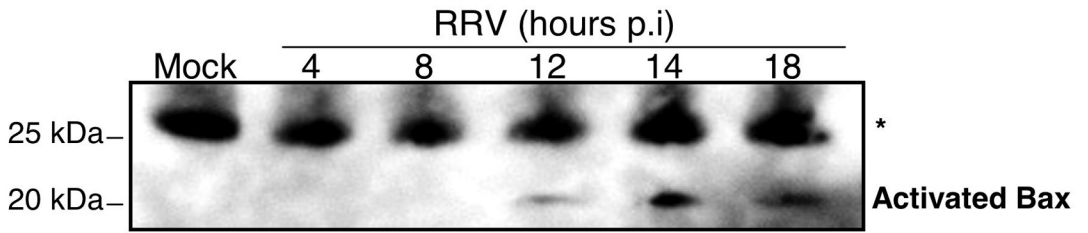
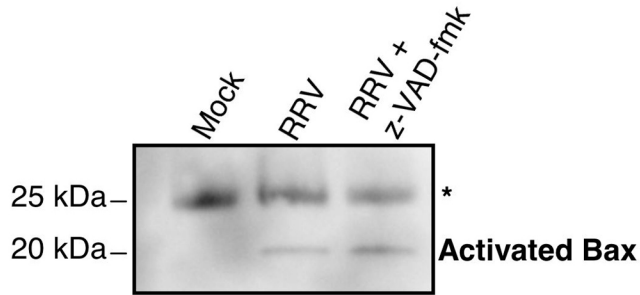
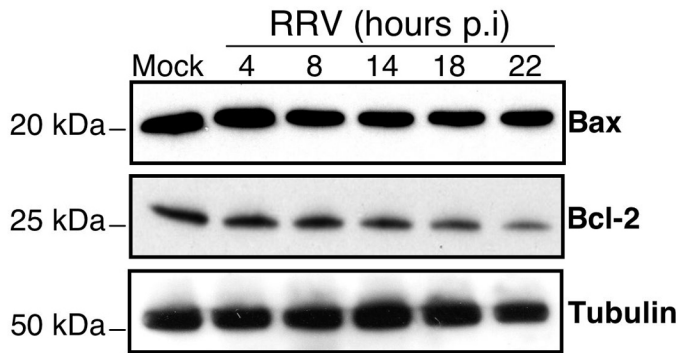
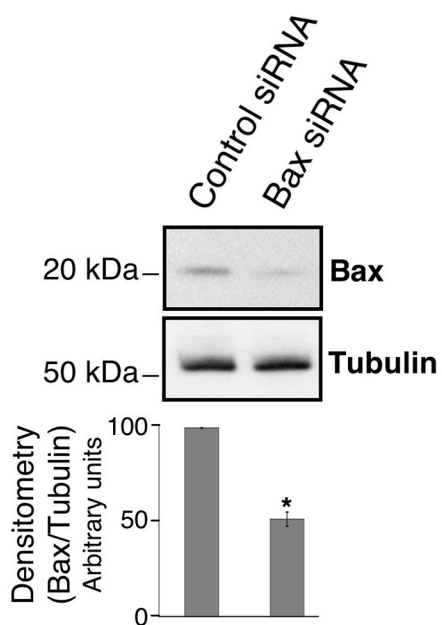
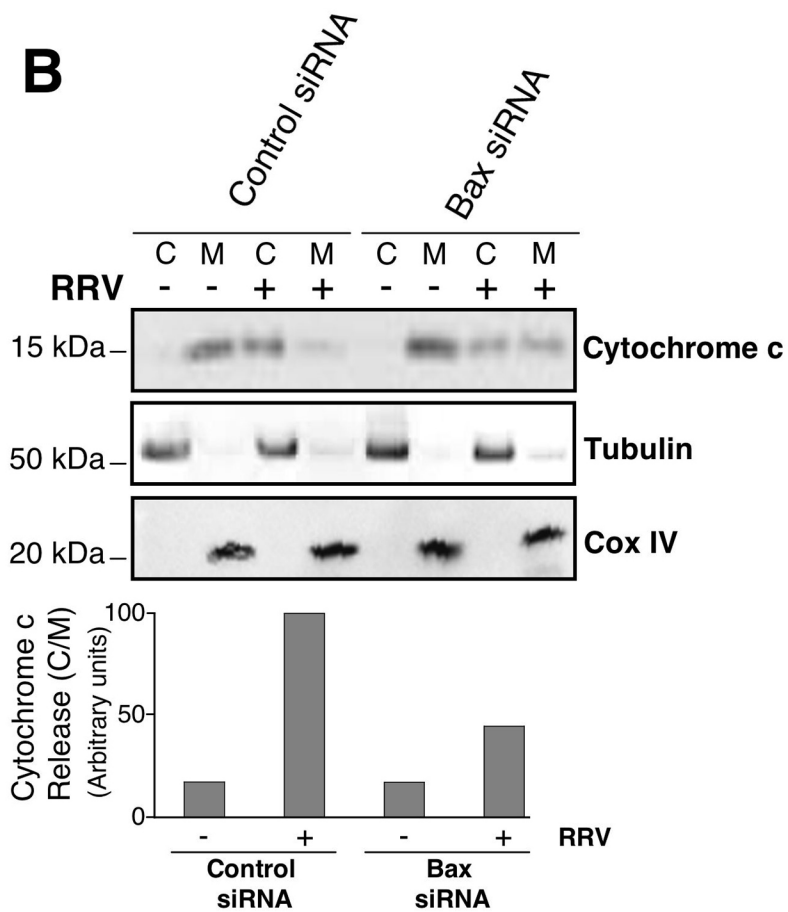
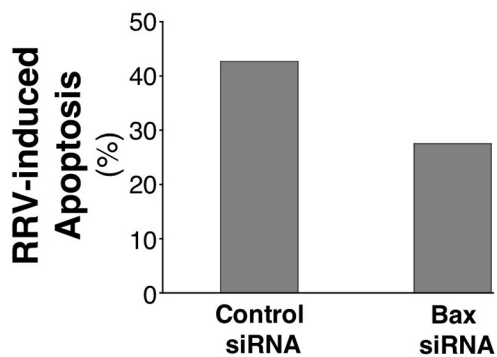


Figure 2

A**B****Figure 3**

A**B****Figure 4**

A**B****C****Figure 5**

A**B****C****Figure 6**